• Basic Research •

Tear proteomics reveals biomarkers for visual field progression in normal-tension glaucoma

Le-Wei Tang[1,2,3], Hui-Yan Mao[1,2], Mei-Min Lin[1,2], Si Zhu[1,2], Qiang-Jie Huang[1,2], De-Fu Chen[1,2], Wei-He Zhou[1,2], Yuan-Bo Liang[1,2,3]

[1]The Eye Hospital of Wenzhou Medical University, Wenzhou 325027, Zhejiang Province, China
[2]National Clinical Research Center for Ocular Diseases, Wenzhou 325027, Zhejiang Province, China
[3]Glaucoma Research Institute of Wenzhou Medical University, Wenzhou 325027, Zhejiang Province, China
Co-first Authors: Le-Wei Tang and Hui-Yan Mao
Correspondence to: Yuan-Bo Liang. National Clinical Research Center for Ocular Diseases, Eye Hospital, Wenzhou Medical University, No. 270, Xue Yuan Xi Road, Wenzhou 325027, Zhejiang Province, China. yuanboliang@wmu.edu.cn
Received: 2025-06-11 Accepted: 2025-08-25

Abstract

● **AIM:** To identify early biomarkers associated with glaucomatous visual field (VF) progression in patients with normal-tension glaucoma (NTG).

● **METHODS:** This study included patients were divided into two groups based on disease progression status. Tear samples were collected for proteomic analysis. Data-independent acquisition (DIA) mass spectrometry combined with bioinformatic analyses was performed to identify and validate potential protein biomarkers for NTG progression. Additionally, differentially expressed proteins (DEPs) were evaluated using mediating effect models and receiver operating characteristic (ROC) curve analysis.

● **RESULTS:** A total of 19 patients (20 eyes) with NTG participated in this study, including 10 patients (4 males and 6 females; 10 eyes) in the progression group with mean age of 67.70±9.03y and 10 patients (4 males and 6 females; 10 eyes) in the non-progression group with mean age of 68.60±7.58y. A total of 158 significantly differentially expressed proteins were detected. UniProt database annotation identified 3 upregulated proteins and 12 downregulated proteins. Kyoto Encyclopedia of Genes and Genomes (KEGG) pathway analysis showed that these DEPs were mainly enriched in pathways such as oocyte meiosis. Gene Ontology (GO) enrichment analysis revealed functional clusters related to cellular processes. Weighted gene co-expression network analysis (WGCNA) indicated that the core proteins were primarily involved in the neurodegeneration-multiple diseases pathway and cellular processes. Mediating effect analysis identified PRDX4 (L) as a potential protein biomarker. ROC curve analysis showed that GNAI1 had the largest area under the curve (AUC=0.889).

● **CONCLUSION:** This study identifies 15 differentially expressed proteins in the tear fluid of NTG patients, including PRDX4 (L). PRDX4 (L) plays a key role in oxidative stress.

● **KEYWORDS:** normal-tension glaucoma; tears; proteomics; biomarkers; visual field progression
DOI:10.18240/ijo.2026.01.01

Citation: Tang LW, Mao HY, Lin MM, Zhu S, Huang QJ, Chen DF, Zhou WH, Liang YB. Tear proteomics reveals biomarkers for visual field progression in normal-tension glaucoma. *Int J Ophthalmol* 2026;19(1):1-10

INTRODUCTION

Glaucoma is a chronic neurodegenerative disease characterised by retinal ganglion cell and visual field (VF) loss and is the leading causes of irreversible blindness, with approximately 60 million patients worldwide suffering from glaucomatous disease[1]. Elevated intraocular pressure (IOP) is commonly considered the primary risk factor for glaucoma[1]. However, normal-tension glaucoma (NTG), a dominant subtype of primary open angle glaucoma, paradoxically presents with characteristic glaucomatous optic neuropathy and corresponding VF impairments despite normal IOP[2].

In China, NTG accounts for a high proportion of primary open angle glaucoma cases[3-5]. It is even more worrying that the consultation rate of patients with NTG is low[6], most patients have already progressed to the middle or late stage by the time they seek medical treatment[7] due to the insidious of neurodegenerative progression, thus missing the optimal treatment period. Additionally, the progression rate of NTG is highly variable, with reported annual mean deviation declines ranging from -0.2 to -2 dB in the Collaborative Normal Tension Glaucoma Study[8] and -0.69 to -1.17 dB in prior research[9]. Currently, structural parameters, such as retinal nerve fiber layer (RNFL) and macular ganglion cell-

inner plexiform layer thickness measured, vascular metrics and peripapillary capillary vessel density are used in the diagnosis of NTG[10-12]. These indicators provide some basis for NTG assessment but have limitations in fully capturing the complexity of disease progression. RNFL thickness measured by optical coherence tomography may show minimal changes in the very early stage, making it difficult to distinguish from physiological variations[10]. Optical coherence tomography angiography-detected microvasculature dropout and peripapillary capillary vessel density are affected by image quality, which may interfere with the identification of early microvascular abnormalities[11-12]. Given the highly variable progression rate of NTG and the limitation of current methods, the use of effective screening strategies to identify patients with rapid progression early and intervene aggressively is of great significance for the preservation of visual function in patients with NTG.

The main focus of clinical proteomics is the discovery of new protein or peptide biomarkers associated with a disease. Over the past decade, clinical proteomics has become a popular research topic in the field, and major breakthroughs in analytical techniques in terms of assay sensitivity have enabled the quantitative analysis of tiny samples of substances such as body fluids that were previously difficult to measure. Proteomics can lead to the discovery of potential biomarkers for ocular and systemic diseases through the use of noninvasive techniques for studying protein levels in tear fluid. Furthermore, emerging mass spectrometry technologies enable the determination of deep proteomic signatures, thereby increasing the sensitivity of the analysis. In addition, faster collection speeds and noninvasive collection methods have made tear fluid a potential disease biomarker in ophthalmology. Current studies on glaucomatous tear proteomics have focused on differences in the tear proteins of healthy and glaucomatous patients. Pieragostino *et al*[13] used the liquid chromatography-mass spectrometry (LC-MS) technique to examine differences in the tear protein levels of healthy individuals and patients with untreated primary open angle glaucoma, and they identified 27 differential proteins. However, no studies have focused on biomarkers of the VF progression in NTG. Moreover, due to the small volume of tears collected, analysis is often performed with mixed samples, which is highly likely to mask interindividual differences.

Therefore, the present study analysed the differences in tear protein composition in progression and non-progression patients with NTG using a very small amount proteomics approach and correlated it with the clinical data. The aim of this study was to find early biomarkers of glaucomatous VF progression in order to provide a basis for the early diagnosis and treatment of patients.

PARTICIPANTS AND METHODS

Ethical Approval This study adhered to the Declaration of Helsinki and was approved by the Ethics Committee of the Eye Hospital of Wenzhou Medical University [approval number KYK (2018) 34]. All participants signed an informed consent form the study began and voluntarily agreed to participate in the study.

Participants All study participants were from the NTG cohort at the Eye Hospital of Wenzhou Medical University[14]. NTG was defined as follows[15]: 1) open anterior chamber angles verified by gonioscopy; 2) median untreated IOP readings less than 21 mm Hg on six different occasions, with no single reading exceeding 24 mm Hg; 3) the presence of glaucomatous optic neuropathy based on disc photographs (vertical cup/disc ratio (C/D) >0.7, vertical C/D asymmetry >0.2, or neural rim tissue <0.1, or localized or diffuse RNFL defects on fundus photography); 4) two or more glaucomatous VF defects that are repeatable and corresponding at baseline; 5) defects in optic nerve and VF not explained by any other medical conditions. In our study, the participants met the following inclusion criteria: 1) patients aged 40 years of age or older; 2) patients with no systemic diseases; 3) patients with the ability to fully understand Chinese; 4) patients with a diagnosis of NTG in at least one eye; 5) patients with no history of ocular surgery, trauma or recent infection. Then we divided them into the progression group and the non-progression group based on whether there was VF defect progression (three or more points in three consecutive VF examinations deteriorated compared with the baseline).

Patients that met any of the following exclusion criteria were not included in the study: 1) patients with a history of intraocular surgery or intravitreal treatment; 2) patients who received systemic or topical hormone therapy within a week; 3) patients with an eye infection, an eye tumour, ocular surface diseases, human immunodeficiency virus (HIV) infection or retinopathy other than glaucoma; 4) patients with autoimmune or neurological diseases; 5) patients with ocular surface disease.

Examinations The participants' routine ophthalmic examinations included visual acuity, dioptre, corneal thickness, the Humphrey VF (24-2), fundus photography, anterior segment optical coherence tomography and Goldmann tonometer testing. In accordance with the Early Manifest Glaucoma Trial-guided[16] progression analysis criteria, a participant was considered to have VF defect progression if three or more points in three consecutive VF examinations deteriorated compared with the baseline.

Tear Collection To collect 10 μL of tears, each participant was asked to tilt their head to one side, and a capillary tube was placed at the lower cul-de-sac of a randomly selected eye. The procedure was performed as gently as possible to minimise

reflexive tearing. The duration of tear collection did not exceed 5min.

The tear sample was transferred into a 0.5 mL Eppendorf tube using a small pump. Next, it was centrifuged at 10 000 rpm in 4℃ for 10min to remove cell debris. Then, the tears were transferred into another Eppendorf tube without disturbing the pellet. The Eppendorf tube containing the tears were sealed with parafilm and stored in a -80℃ freezer until the analysis was conducted.

Protein Extraction and Digestion All samples were prepared using the in-solution digestion method. Briefly, the detergent (Sodium dodecyl sulfate, with a final concentration of 20 mmol/L) was added to each sample and incubated for 2h at 37℃. After cooling to room temperature, an alkylating agent was added into the mixture to block reduced cysteine residues (with a final concentration of 40 mmol/L) and mixed at 600 rpm for 1min. The mixture was incubated for 30min in darkness. Agent C (TCEP reducing Agent, for breaking disulfide bonds in proteins, 3 μL) and agent D (IAA alkylating agent, for blocking the free thiol groups after reduction, 5 μL) were sequentially added. The reaction was terminated by heating to 95℃ and digested with trypsin for 2h at 37℃. The resulting peptides of each sample were desalted, concentrated *via* vacuum centrifugation and reconstituted in 0.1% (v/v) formic acid. The peptide content was estimated using UV light spectral density at 280 nm. For the data independent acquisition (DIA) experiments, the sample was spiked with indexed retention time calibration peptides (400 ng/sample). All proteomic analyses were technically helped by Shanghai Applied Protein Technology.

Mass Spectrometry Assay for Data Independent Acquisition DIA analysis was performed using a timsTOF Pro mass spectrometer (Bruker) coupled with a nanoElute liquid chromatography system (Bruker) in DIA mode for 60min. The mass spectrometer operated in positive ion mode. Collecting ion mobility MS spectra over m/z 100–1700.32 windows for single 100ms TIMS scans were defined according to the m/z-ion mobility plane.

Mass Spectrometry Data Analysis DIA data were analysed with Spectronaut™ 14.4.200727.47784. The main software parameters were set as follows: the retention time prediction type was dynamic indexed retention time, interference on MS2 level correction was enabled and cross-run normalisation was enabled. Results were filtered based on a Q value cutoff of 0.01 (equivalent to FDR <1%).

Bioinformatic Analysis

Cluster analysis Hierarchical clustering used Cluster 3.0 software (http://bonsai.hgc.jp/mdehoon/software/cluster/software.htm) and Java TreeView software (http://jtreeview.sourceforge.net). In the hierarchical clustering, Euclidean distance was used as a similarity measure, and average linkage clustering was used for clustering (clustering uses the centroids of the observations). Dendrograms were often accompanied by heat maps as visual aids.

Subcellular localisation A multiclass SVM classification system called CELLO (http://cello.life.nctu.edu.tw/) was used to predict protein subcellular localisation.

Domain annotation Protein domain signatures were identified by searching the Pfam database for protein sequences using InterProScan software.

Gene ontology annotation Homologous sequences of differentially expressed proteins were found using NCBI BLAST+ client (ncbi-blast-2.2.28+-win32.exe) and InterProScan locally. Blast2 gene ontology (GO) performed GO term mapping and sequence annotation, while R scripts plotted GO annotation results.

Kyoto Encyclopedia of Genes and Genomes annotation A Kyoto Encyclopedia of Genes and Genomes (KEGG) orthology databank (http://geneontology.org/) was searched to obtain the KEGG orthology identifications for the studied proteins, which were subsequently mapped to pathways in KEGG.

Enrichment analysis Fisher's exact test was used for the enrichment analysis, with all quantified proteins the background dataset. The *P*-values derived from multiple tests were further adjusted using the Benjamini-Hochberg correction. A *P*-value of less than 0.05 was considered significant for the functional categories and pathways.

Principal component analysis After being normalised to total peak intensity, the processed data were uploaded to SIMCA-P version 14.1 (Umetrics, Umea, Sweden) for multivariate data analysis, including pareto-scaled principal component analysis (PCA).

Weighted gene co-expression network analysis The weighted gene co-expression network analysis (WGCNA) package in R package (Version 1.69) was used to identify distinct protein modules. A weighted protein co-expression network was generated using the $\log_2$ protein abundance sample matrix. Co-expression modules associated with traits were identified through the following criteria: the closer the correlation value is to ±1 and the correlation test *P* values less than 0.05.

Statistical Analysis Statistical analysis was conducted using SPSS software version 26.0 for Windows (IBM Corp., Armonk, NY, USA). Continuous variables were shown as mean±standard deviation (SD). Comparisons between groups were performed using an independent samples *t*-test. Variables not conforming to a normal distribution were expressed as median values (IQRs). The statistical significance of the changes in protein abundance were determined using the nonparametric Student's *t*-test with Bonferroni multiple testing correction. Changes with a two-tailed $P<0.05$ were considered

Table 1 Demographics and clinical of progression group and non-progression group mean±SD

Parameters	Progression (*n*=10)	Non-progression (*n*=10)	*P*
Age, y	67.70±9.03	68.60±7.58	0.812
Gender (M/F)	4/6	4/6	NA
Baseline IOP, mm Hg	15.33±2.77	14.25±2.43	0.368
Mean IOP, mm Hg	14.95±2.89	14.75±2.38	0.753
Vertical C/D	0.77±0.07	0.79±0.11	0.673
Baseline RNFL thickness, μm	73.50±14.88	70.50±9.49	0.597
Mean deviation, dB	-7.19±5.97	-10.29±6.21	0.270

IOP: Intraocular pressure; SD: Standard deviation; C/D: Cup/disc ratio; RNFL: Retinal nerve fiber layer.

statistically significant. The predictive ability of the differential proteins was evaluated in terms of the receiver operating characteristic (ROC) curve calculated by the area under the curve (AUC), sensitivity and specificity. ROC curves were performed using R (R Core Team 2022).

RESULTS

Demographic and Clinical Data A total of 19 patients (20 eyes) with NTG participated in this study, including 10 (10 eyes) patients in the progression group and 10 patients (10 eyes) in the non-progression group. The male-to-female ratio in both groups was 4:6. The average age (67.70±9.03, 68.60±7.58y), baseline IOP (15.33±2.77, 14.25±2.43 mm Hg), average IOP (14.95±2.89, 14.75±2.38 mm Hg), C/D (0.77±0.07, 0.79±0.11), baseline RNFL thickness (73.50±14.88, 70.50±9.49 μm) and mean deviation (-7.19±5.97, -10.29±6.21 dB). No statistical differences were found for the above indicators (Table 1).

DIA Analysis of the Tear Proteome

Quantitative analysis of the identified proteins Of the total number of identified proteins, 5907 were expressed in both groups, 240 were only found in the non-progression group, and 264 were only found in the progression group. Figure 1A showed there was no outlier sample in the protein abundance analysis and the quality of sample was reliable for further analysis. According to the principal component analysis (PCA), there was no significant difference within the two groups but significant differences between the groups (Figure 1B) The Venn diagram in Figure 1C presents the distribution of the proteins identified in the two groups. The quantitative signals of the identified proteins in all samples are displayed in the form of heat maps in Figure 1D.

Expression difference analysis of the identified proteins In the screening of the significantly differential proteins, $\log_2$-transformed fold change (FC) was expressed as greater than the upratio fold (upregulated greater than the upratio fold or down adjusted less than downratio times), and a $P<0.05$ was used as the standard. A statistically significant increase in 102 proteins and a statistically significant decrease in 56 proteins were observed in the progression and non-progression groups in the tear samples.

Figure 2A shows volcano plots created based on the expression of two factors: FC and *P*-value. The significantly downregulated proteins are labelled in blue (FC<0.67 and $P<0.05$), and the significantly upregulated proteins are labelled in red (FC>1.5 and $P<0.05$). The undifferentiated proteins are labelled in grey, and the top 10 with the most significant upregulated protein differences are labelled. In addition, the cluster analysis results in Figure 2B shows that the difference of differentially expressed proteins in the two groups was obvious.

UniProt Database Analysis After screening and removing peptides and other proteins without biological functions, 15 differential proteins (3 upregulated and 12 downregulated proteins) were included in the analysis. Table 2 lists the UniProt IDs, the genes and names of the protein and their protein classes. All catalytic activity proteins, including peroxiredoxin-4, were downregulated in the progression group compared to the non-progression group. Similarly, there were binding and molecular function regulator proteins, such as plasminogen activator inhibitor. The 15 differentially expressed proteins also be shown in boxplots in Figure 2C.

Functional Analysis of the Identified Proteins The top 20 domains were listed in Figure 3A and 3B from Domain analysis. Notably, immunoglobulin V-set domain ranked first and was contained by 119 proteins which was far more than other domains in the amount. Subcellular localisation analysis shows that the differentially expressed proteins were mainly from extracellular, nuclear and cytoplasmic (Figure 3C). KEGG analysis indicated that pathways such as parathyroid hormone synthesis, secretion and action, purine metabolism, one carbon pool by folate, and oocyte meiosis were significantly enriched (Figure 3D). The results of GO analysis shows that the main biological processes were cellular process, metabolic process, biological regulation, and molecular function was binding, catalytic activity, molecular function regulator, and cellular component was cell part, cell, organelle, membrane (Figure 3E).

WGCNA The WGCNA was used to identify the modules (Figure 4). A total of 6179 modules were identified by WGCNA (Figure 4A). Then 12 co-expression modules associated with traits were identified and the module-trait relationship heatmap demonstrated the correlations between the module and clinical

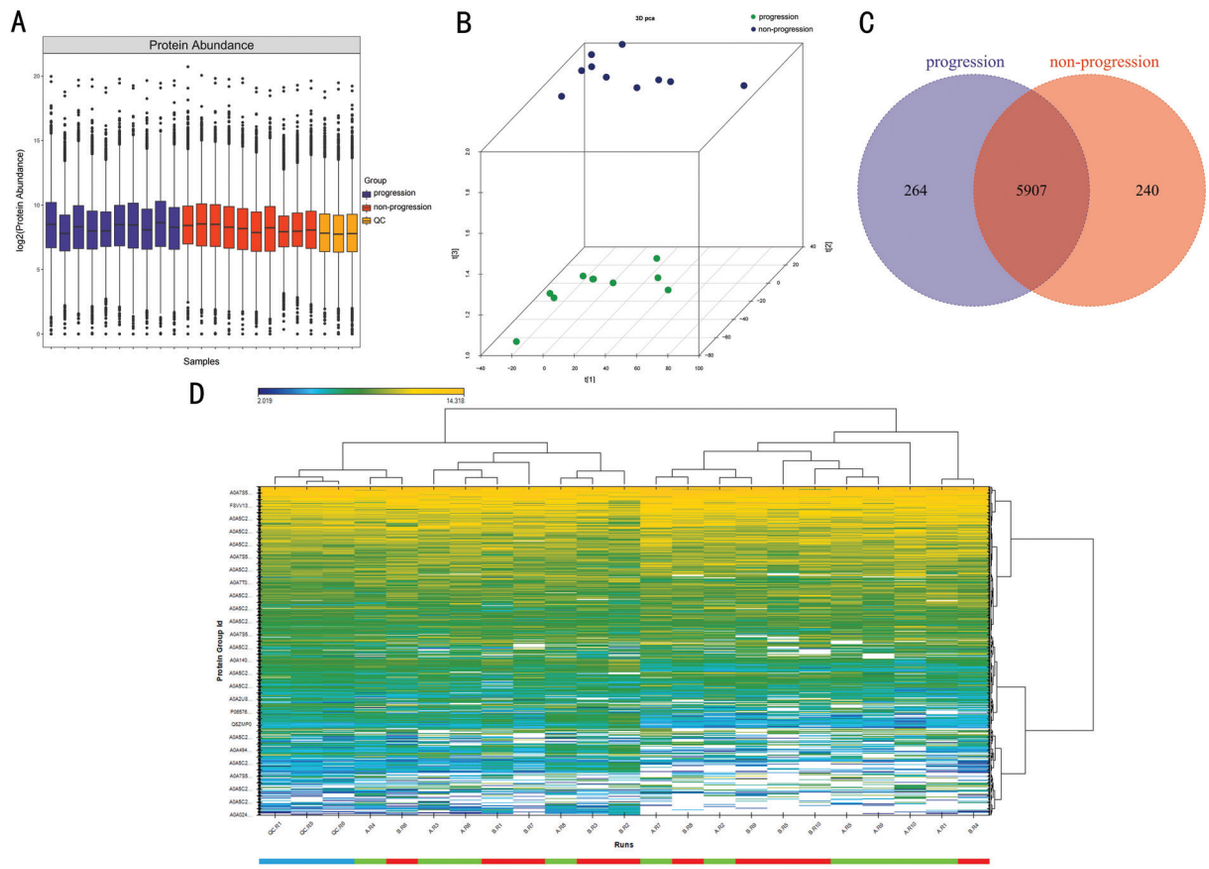

Figure 1 Proteomic data quality assessment and differential expression analysis A: Quality control for samples. The center line shows the median, the box limits represent the upper and the lower quartiles, and the whiskers extend to the largest and smallest values; B: 3D PCA to reflect the variability between and within the sample groups; C: The Venn diagram of differentially expressed proteins; D: Heat map visualization of the identified protein in all sample. The expression of the protein is displayed in different colors, with the darker yellow indicating a stronger signal and the darker blue indicating a stronger signal weak. White means no quantitative information.

traits (Figure 4B). Finally, one markedly expressed modules (turquoise) associated with clinical traits was identified (Figure 4C). KEGG enrichment analysis found that the pathways of neurodegeneration-multiple diseases, Parkinson disease, Alzheimer disease, regulation of actin cytoskeleton, PI3K-Akt signalling pathway and Human papillomavirus infection were significantly enriched in the turquoise module (Figure 4D). GO enrichment of the turquoise module showed that it was involved in the cellular response and primarily distributed in the cellular region (Figure 4E).

Analysis of the mediating effect among protein, clinical data and glaucoma progression Baseline clinical data were used as the independent variables; glaucoma progression was used as the dependent variable; and tear proteomic indicators were used as mediation variables. The logistic regression results showed that the baseline clinical data had no statistically significant effect on glaucoma progression. Combined with the results of the linear regression model with the baseline clinical data as the independent variables and the tear proteomics indicators as the dependent variables and the results of the logistic regression model with the baseline clinical data, the tear proteomic indicators as the independent variables and glaucoma progression as the dependent variable showed that the baseline IOP had an effect on glaucoma progression through PRDX4 (L). The indirect effect was -0.007 (P=0.024), and the direct effect was 0.013 (P<0.001). Thus, PRDX4 (L) had a masking effect on the baseline IOP (Figure 5A).

Prediction of Progression using Proteomics ROC analysis was performed to assess the sensitivity and specificity of each protein in detecting the progression of glaucoma. The AUC values of the 15 proteins are shown in Table 2. Figure 5B shows the ROC curves of the four proteins with the largest AUC values for clinical prediction. The protein with the largest AUC value was GNAI1 (0.889).

DISCUSSION

Body fluids, especially blood, saliva, urine, cerebrospinal fluid and sweat, are sources of biomarkers for the diagnosis of human diseases. Tear fluid is an emerging biomarker source with unique advantages in disease diagnosis and treatment. Tears contain more than 1500 measurable proteins in concentrations ranging from 6 to 11 mg/mL. In contrast, saliva has a protein concentration range of 0.4–4.4 mg/mL[17],

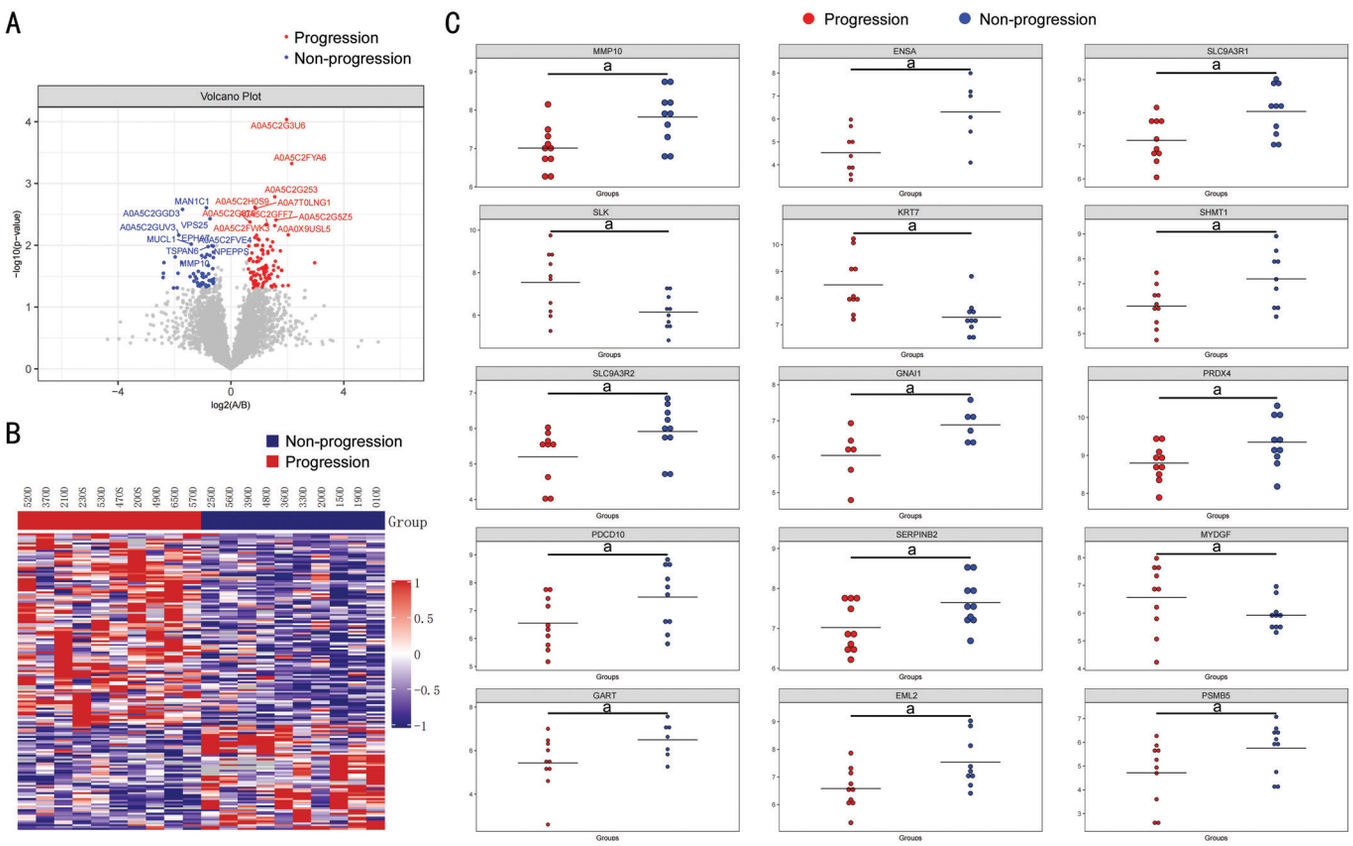

Figure 2 Differentially expressed proteins between progression and non-progression groups A: A volcano plot visualizing the differentially expressed proteins between progression group and non-progression group. In volcano plots, red and blue spots represent differentially expressed proteins (fold change >1.5 or <0.67, *P* value <0.05), and black spots represent the proteins changing insignificantly. B: Comparisons of the heatmaps of the differentially expressed proteins among the progression group and non-progression group. Red and blue represent the expression of this differential protein in different samples. [a]*P*<0.05. C: Boxplot visualizing the differentially expressed proteins after screening and removing peptides and other proteins without biological functions between progression group and non-progression group.

Table 2 List of protein groups showed differential abundance in progression and non-progression groups

UniProt Ids	Gene	Protein description	Protein class	*P*	AUC
Upregulated in the progression group compared to the non-progression group					
Q9H2G2	*SLK*	STE20-like serine/threonine-protein kinase		0.026	0.77
P08729	*KRT7*	Keratin, type II cytoskeletal 7	Structural molecule activity	0.029	0.87
Q969H8	*MYDGF*	Myeloid-derived growth factor		0.043	0.70
Downregulated in the progression group compared to the non-progression group					
Q13162	*PRDX4*	Peroxiredoxin-4	Catalytic activity	0.039	0.76
P05120	*SERPINB2*	Plasminogen activator inhibitor 2	Binding; catalytic activity; molecular function regulator	0.042	0.76
P63096	*GNAI1*	Guanine nucleotide-binding protein G(i) subunit alpha-1	Binding; catalytic activity	0.037	0.89
P09238	*MMP10*	Stromelysin-2	Catalytic activity	0.014	0.82
P28074	*PSMB5*	Proteasome subunit beta type-5	Catalytic activity	0.047	0.76
P22102	*GART*	Trifunctional purine biosynthetic protein adenosine-3	Catalytic activity	0.044	0.80
O14745	*NHERF1*	Na(+)/H(+) exchange regulatory cofactor NHE-RF1	Binding; molecular adaptor activity	0.016	0.81
Q15599	*NHERF2*	Na(+)/H(+) exchange regulatory cofactor NHE-RF2	Binding; molecular adaptor activity	0.037	0.81
Q9BUL8	*PDCD10*	Programmed cell death protein 10	Binding	0.040	0.77
O95834	*EML2*	Echinoderm microtubule-associated protein-like 2	Binding	0.044	0.79
D3DXC9	*SHMT1*	Serine hydroxy methyltransferase		0.032	0.77
A6NMQ3	*ENSA*	Endosulfine alpha		0.015	0.87

AUC: Area under the curve.

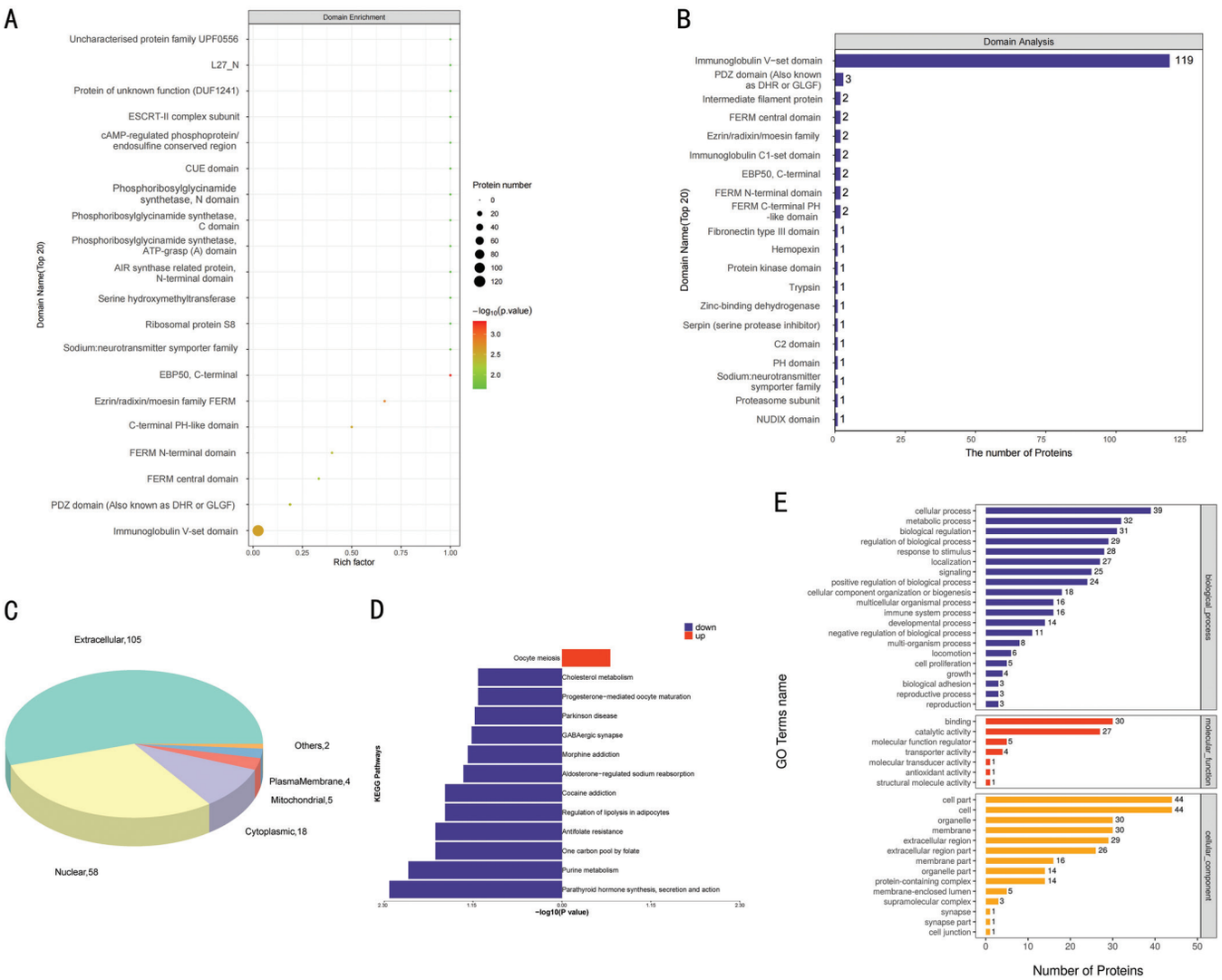

Figure 3 Functional characterization of differentially expressed proteins between progression and non-progression group A, B: The Domain analysis of differentially expressed proteins between progression group and non-progression group. C: Subcellular localization analysis of differentially expressed proteins. D: Analysis of KEGG pathway enrichment revealed the pathway of differentially expressed proteins. E: GO functional enrichment analysis of differentially expressed proteins between progression group and non-progression group. Functional classification is divided into biological process, molecular function and cellular component. KEGG: Kyoto Encyclopedia of Genes and Genomes; GO: Gene ontology.

and sweat contains no proteins[18]. Since molecules can easily diffuse from blood into tears, biomarker levels in tears are comparable to those in blood, making tears a reliable and noninvasive source of biomarkers. In addition, tear fluid, one of the most commonly used body fluids, is characterised by its ease of collection, rapid updating and ability to carry rich biological information[19].

Tear proteomic studies have shown that protein types and levels in tear samples are influenced by a variety of factors, including tear sampling methods (Schirmer strips, eye rinsing, and glass capillary tubes[20-21]), protein determination methods (Bradford[22] and Lowry methods[23]), the type of tears collected (reflex and non-stimulated tears), diurnal variations[24], gender[25], age[26] and whether or not the eyes are closed[27]. The three most commonly used tear sampling methods are cellulose sponges, capillary tubes and Schirmer test strips. Of these, the capillary method is less invasive, and it destroys fewer proteins during sample recovery[28]. To prevent the collected tears from being irritating, the collection time for each of the participants in the present study was less than 5min. Blood and atrial fluid samples are often collected from glaucoma patients because they can provide additional information about the health of the eye as well as the whole body. However, they are invasive, and many patients are sceptical about them. Due to advances in mass spectrometry, noninvasive sampling methods have made tear analysis an attractive option for disease diagnosis and monitoring.

In the present study, 15 differential proteins were identified in progression and non-progression patients by analysing tear samples from 20 individual eyes. The sensitivity and specificity

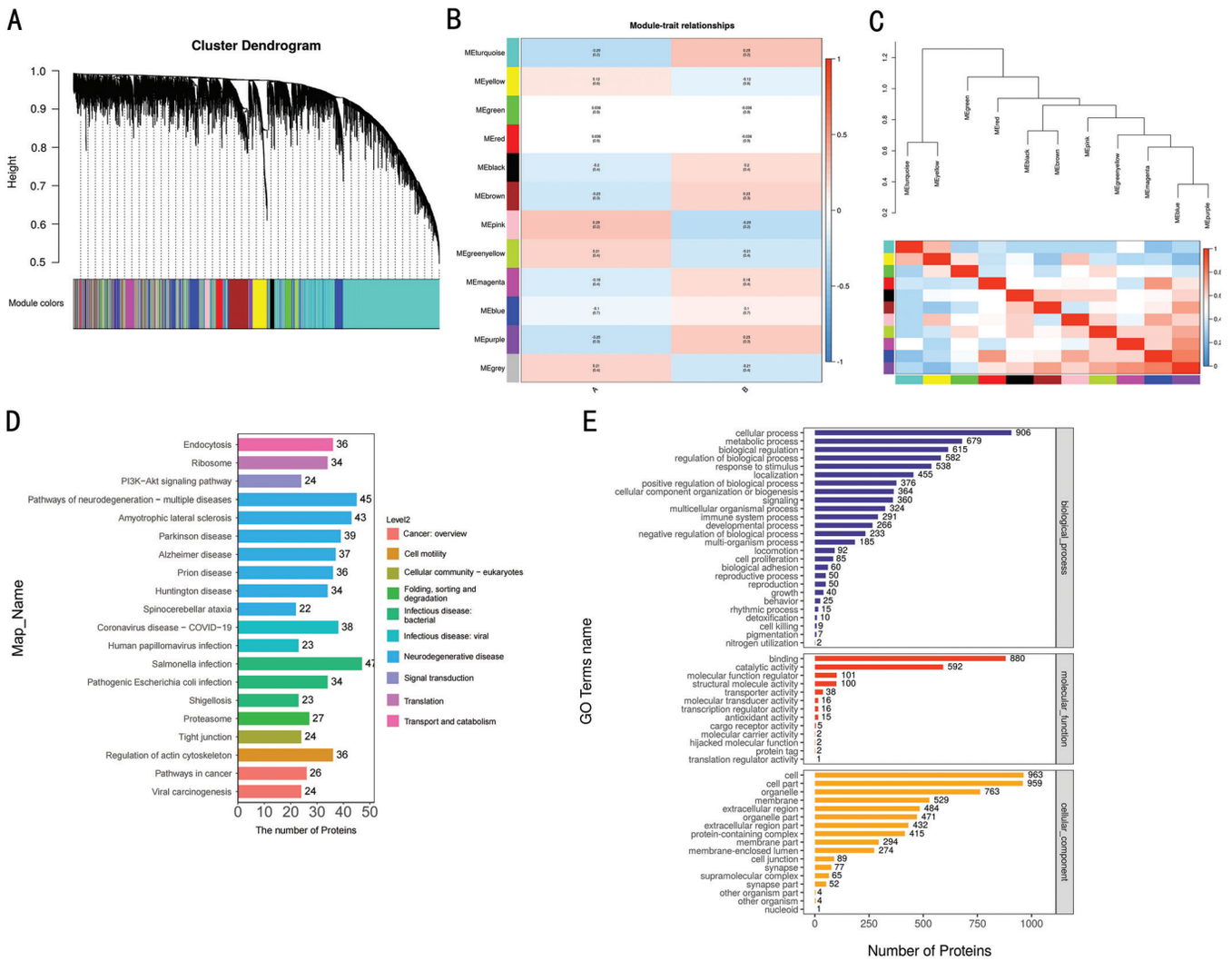

Figure 4 Integrated analysis of protein expression profiles and functional enrichment A: Hierarchical clustering and module detection based on protein/peptide expression patterns. The dendrogram shows the clustering of proteins/peptides and the colors below represent the identified modules. B: Module-trait relationships for various clinical traits. The module name is shown on the left side of each cell, and the correlations between the module eigengene and each trait are displayed. The color-coded table indicates the strength of the correlations. C: Dendrogram of consensus module eigengenes and heatmap of module adjacencies. The heatmap shows the correlations (positive or negative) between the identified modules. D: KEGG constructed using the top 20 hub proteins in the turquoise modules. E: GO enrichment analyses of the differentially expressed proteins in the two groups. KEGG: Kyoto Encyclopedia of Genes and Genomes; GO: Gene ontology.

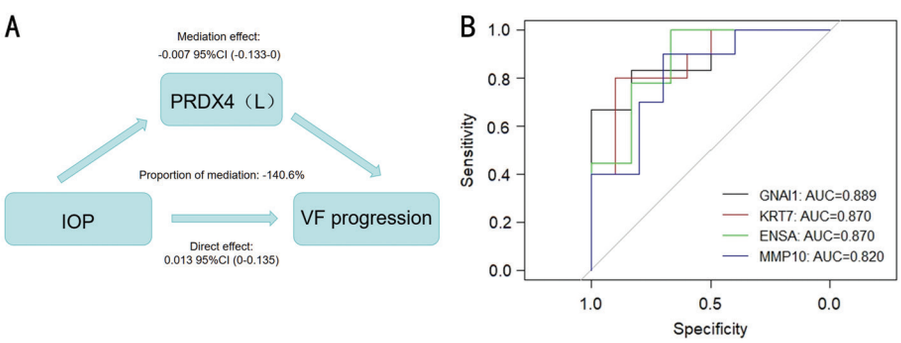

Figure 5 Proteomics based mediation analysis and clinical prediction of glaucoma progression A: Proteomics parameters mediation models of the relationship between IOP and VF progression; B: ROC for clinical prediction of the progression of glaucoma based on the proteomics (The figure shows the four proteins with the largest AUC area for clinical prediction). AUC: Area under the curve; IOP: Intraocular pressure; VF: Visual field; ROC: Receiver operating characteristic.

of these proteins in predicting glaucomatous progression were analysed using ROC curves. The AUC values for these proteins were greater than 0.7, and the AUC values for GNAI1, KRT7 and ENSA were all greater than 0.85.

Pieragostino *et al*[13] found 27 tear protein differences between healthy individuals and patients with untreated primary open angle glaucoma. Ten of those proteins (IGJ, ALB, HSPB1, CST4, PIGR, ACTB, ACTG1, TF, PIP and PROL1) were also detected in the present study. However, no statistically significant differences in any of the aforementioned proteins were detected because both groups in the present study were comprised of glaucoma patients.

Guanine nucleotide-binding proteins (G proteins) act as transducers downstream of G protein-coupled receptors in a number of signalling cascades. α-chains contain guanine nucleotide-binding sites and alternate between active Guanosine triphosphate-binding states and inactive Guanosine diphosphate-binding states[29]. GNAI1 has been implicated in a number of pathways, such as glutamatergic metabolism, Parkinson's disease, Ca^{2+} channels and the cGMP-PKG signalling pathway, all of which are relevant to glaucoma pathomechanisms[30].

Combined with the clinical data, IOP and PRDX4 (L) were strongly correlated with VF progression, and PRDX4 (L) had a masking effect. In other words, the downregulation of PRDX4 (L) increased the likelihood of VF progression. Thiol-specific peroxidase catalysed the reduction of hydrogen peroxide and organic hydroperoxides to water and alcohols, respectively. It played a role in cell protection against oxidative stress by detoxifying peroxides and acting as a sensor of hydrogen peroxide-mediated signalling event[31]. It regulated the activation of NF-kappa-B in the cytosol by modulating I-kappa-B-alpha phosphorylation[32].

Its reduced expression deprived the cells of protection from oxidative stress, which caused optic nerve damage and ultimately led to VF progression. Analysis of the reduced expression of PRDX4 (L) revealed that the patients had higher levels of IOP, which led to progressive damage to the optic nerve. In patients with NTG, IOP remains an important factor in optic nerve damage even if the corresponding target IOP range is not reached, although all IOPs are below 21 mm Hg. Similarly, disruption of the redox system imbalance has been shown to play an important role in the pathogenesis of glaucoma in experimental studies, and it is clear that ROS can effectively protect retinal ganglion cells in mice in a high IOP model[33]. Furthermore, oxidative stress plays an important role in glaucomatous optic nerve injury, and reduced PRDX4 (L) expression may be a potential biomarker of VF progression in patients with NTG. In the future, antioxidative stress-related treatment may become an important strategy for optic nerve protection in patients with NTG.

The present study had several main limitations. First, the sample size was small. Although, through regular follow-ups over 10y, we had built an NTG cohort of about 200 people, of which about 90 patients showed VF progression, fewer patients met our inclusion criteria, were willing to cooperate and were able to collect samples successfully. Second, the tear collection methods could have been optimised. Although the capillary method we used is considered less invasive and destroys fewer proteins during sample recovery, it is more difficult to collect a sufficient amount of tear fluid in 5min in older patients. As such, this method is not suitable for future clinical applications. In summary, the present study compared tear samples from patients with progression and non-progression NTG vision using a proteomic approach. The study identified 15 differential proteins, including PRDX4 (L), which plays an important role in oxidative stress and may be a potential biomarker.

ACKNOWLEDGEMENTS

Foundations: Supported by The Eye Hospital of Wenzhou Medical University (No.KYQD20220304); The Fifth Batch of Provincial Ten Thousand Personnel Program Outstanding Talents Funding (No.474092204); Innovative Talents and Teams (2024) - The Fifth Batch of Funding Funds for Scientific and Technological Innovation Leading Talents Under the Provincial Ten Thousand Personnel Program (No.4240924003G); The Key R&D Program of Zhejiang (No.2022C03112).

Conflicts of Interest: Tang LW, None; **Mao HY,** None; **Lin MM,** None; **Zhu S,** None; **Huang QJ,** None; **Chen DF,** None; **Zhou WH,** None; **Liang YB,** None.

REFERENCES

1 Jayaram H, Kolko M, Friedman DS, *et al*. Glaucoma: now and beyond. *Lancet* 2023;402(10414):1788-1801.

2 Leung DYL, Tham CC. Normal-tension glaucoma: current concepts and approaches-a review. *Clin Exp Ophthalmol* 2022;50(2):247-259.

3 Liang YB, Friedman DS, Zhou Q, *et al*. Prevalence of primary open angle glaucoma in a rural adult Chinese population: the Handan eye study. *Invest Ophthalmol Vis Sci* 2011;52(11):8250-8257.

4 Wang YX, Xu L, Yang H, *et al*. Prevalence of glaucoma in North China: the Beijing eye study. *Am J Ophthalmol* 2010;150(6):917-924.

5 He MG, Foster PJ, Ge J, *et al*. Prevalence and clinical characteristics of glaucoma in adult Chinese: a population-based study in Liwan District, Guangzhou. *Invest Ophthalmol Vis Sci* 2006;47(7):2782-2788.

6 Chen DF, Wang CM, Si YQ, *et al*. Natural history and risk factors for glaucoma progression in Chinese patients with normal-tension glaucoma. *Invest Ophthalmol Vis Sci* 2024;65(3):28.

7 Li YB, Jiang JH, Wang NL. A review of epidemiological studies on glaucoma in China. *Zhonghua Yan Ke Za Zhi* 2019;55:634-640.

8 Anderson DR, Drance SM, Schulzer M, *et al*. Natural history of normal-tension glaucoma. *Ophthalmology* 2001;108(2):247-253.

9 Tang LW, Chen L, Ye C, *et al*. Population-based associations between progression of normal-tension glaucoma and Yang-deficient constitution among Chinese persons. *Br J Ophthalmol* 2023;107(1):37-42.

10 Lee JS, Lee K, Seong GJ, *et al*. Clinical predictors of the region of first structural progression in early normal-tension glaucoma. *Korean J Ophthalmol* 2020;34(4):322.

11 Jung Y, Park HL, Shin H, *et al*. Microvasculature dropout and development of normal tension glaucoma in glaucoma suspects: the normal tension glaucoma suspect cohort study. *Am J Ophthalmol* 2022;243:135-148.

12 Chen DF, Wang CM, Zhou WH, *et al*. Progressive peripapillary capillary vessel density loss and long-term visual field progression in Normal tension glaucoma. *Acta Ophthalmol* 2024;102(5):e746-e753.

13 Pieragostino D, Agnifili L, Fasanella V, *et al*. Shotgun proteomics reveals specific modulated protein patterns in tears of patients with primary open angle glaucoma naïve to therapy. *Mol Biosyst* 2013;9(6):1108-1116.

14 Tang JJ, Liang YB, O'Neill C, *et al*. Cost-effectiveness and cost-utility of population-based glaucoma screening in China: a decision-analytic Markov model. *Lancet Glob Health* 2019;7(7):e968-e978.

15 Leung DY, Li FC, Kwong YY, *et al*. Simvastatin and disease stabilization in normal tension glaucoma: a cohort study. *Ophthalmology* 2010;117(3):471-476.

16 Heijl A, Bengtsson B, Hyman L, *et al*. Natural history of open-angle glaucoma. *Ophthalmology* 2009;116(12):2271-2276.

17 Grocholska P, Kowalska M, Bąchor R. Qualitative and quantitative mass spectrometry in salivary metabolomics and proteomics. *Metabolites* 2023;13(2):155.

18 Bennet D, Khorsandian Y, Pelusi J, *et al*. Molecular and physical technologies for monitoring fluid and electrolyte imbalance: a focus on cancer population. *Clin Transl Med* 2021;11(6):e461.

19 Nättinen J, Aapola U, Nukareddy P, *et al*. Clinical tear fluid proteomics-a novel tool in glaucoma research. *Int J Mol Sci* 2022;23(15):8136.

20 Tham ML, Mahmud A, Abdullah M, *et al*. Tear samples for protein extraction: comparative analysis of schirmer's test strip and microcapillary tube methods. *Cureus* 2023;15(12):e50972.

21 Pieczyński J, Szulc U, Harazna J, *et al*. Tear fluid collection methods: Review of current techniques. *Eur J Ophthalmol* 2021;31(5):2245-2251.

22 Coyle PK, Sibony PA, Johnson C. Electrophoresis combined with immunologic identification of human tear proteins. *Invest Ophthalmol Vis Sci* 1989;30(8):1872-1878.

23 Sack RA, Tan KO, Tan A. Diurnal tear cycle: evidence for a nocturnal inflammatory constitutive tear fluid. *Invest Ophthalmol Vis Sci* 1992;33(3):626-640.

24 Zhang XZ, Jie Y. Importance of circadian rhythms in the ocular surface. *Biomolecules* 2024;14(7):796.

25 Wingo AP, Liu Y, Gerasimov ES, *et al*. Sex differences in brain protein expression and disease. *Nat Med* 2023;29(9):2224-2232.

26 Aydin E, Nie S, Azizoglu S, *et al*. What's the situation with ocular inflammation a cross-seasonal investigation of proteomic changes in ocular allergy sufferers' tears in Victoria, Australia. *Front Immunol* 2024;15:1386344.

27 Sack RA, Sathe S, Beaton A. Tear turnover and immune and inflammatory processes in the open-eye and closed-eye environments: relationship to extended wear contact lens use. *Eye Contact Lens* 2003;29(1 Suppl):S80-S82.

28 Castelli S, Arasi S, Pawankar R, *et al*. Collection of nasal secretions and tears and their use in allergology. *Curr Opin Allergy Clin Immunol* 2018;18(1):1-9.

29 Vetter IR, Wittinghofer A. The guanine nucleotide-binding switch in three dimensions. *Science* 2001;294(5545):1299-1304.

30 Villar-Conde S, Astillero-Lopez V, Gonzalez-Rodriguez M, *et al*. Synaptic involvement of the human amygdala in Parkinson's disease. *Mol Cell Proteomics* 2023;22(12):100673.

31 Amatya B, Yang SF, Yu PY, *et al*. Peroxiredoxin-4 and dopamine D5 receptor interact to reduce oxidative stress and inflammation in the kidney. *Antioxid Redox Signal* 2023;38(16-18):1150-1166.

32 Ouyang MZ, Luo ZT, Zhang WJ, *et al*. Protective effect of curcumin against irinotecan-induced intestinal mucosal injury *via* attenuation of NF-κB activation, oxidative stress and endoplasmic reticulum stress. *Int J Oncol* 2019;54(4):1376-1386.

33 Sanz-Morello B, Ahmadi H, Vohra R, *et al*. Oxidative stress in optic neuropathies. *Antioxidants (Basel)* 2021;10(10):1538.